Time-Optimal Attitude Maneuver Planning of a Spacecraft Using Control Moment Gyros in a Roof Array

By Ryosuke SAKAMOTO,[1)] Yasuhiro SYOJI,[1)] Satoshi SATOH,[1)] Ichiro JIKUYA,[2)] and Katsuhiko YAMADA[1)]

[1)]*Osaka University, Japan*
[2)]*Kanazawa University, Japan*

A Control Moment Gyro (CMG) is suitable for a spacecraft actuator that realizes fast attitude manuever due to their high torque capability. However, the computation of the minimum attitude manuever time and its trajectories of a spacecraft with a CMG system is complex. In this study, a method is proposed to estimate an approximate solution of the minimum attitude manuever time and its manuever trajectories in a rest-to-rest maneuver of a spacecraft with a roof-array CMG system. To reduce computational time, analytical solutions are derived for the maximum angular momentum of the CMG system in any direction by using inverse kinematics and approximate calculations of the attitude maneuver trajectory of the spacecraft. The approximate solutions are obtained in a short time and estimate the optimal solutions accurately. Numerical simulations show that the attitude control is possible by following the reference trajectories that are the modified approximate trajectories.

ルーフ配置型CMGによる宇宙機の最適姿勢変更計画

坂本遼介，荘司泰弘，佐藤訓志，軸屋一郎，山田克彦

Control Moment Gyro (CMG) は高出力であることから高速な姿勢変更を要する宇宙機のアクチュエータとして適している．しかしながら，CMG システムを搭載した宇宙機の最短姿勢変更時間とその時の軌道の計算は複雑である．そこで，本研究ではルーフ配置型 CMG システムを搭載した宇宙機の rest-to-rest maneuver における最短姿勢変更時間とその時の姿勢変更軌道の近似解を短時間で概算する手法を提案する．計算時間を削減するために，逆キネマティクスによる計算による任意の方向における CMG システムの最大角運動量の解析解の導出や，宇宙機の最適姿勢変更軌道の近似計算を行った．最短姿勢変更時間の概算値は短時間で得られ，最適解を精度よく推定した．また，数値シミュレーションを用いて，修正した概算軌道を参照軌道とする姿勢変更が可能であることを示した．

Key Words: Spacecraft, Attitude Control, Satellite Scheduling, Agile Maneuver, Control Moment Gyro, Roof Array

1. Introduction

Rapid maneuver of a spacecraft is important for a modern spacecraft to accomplish various demanding space missions, for example, taking more images effectively in a limited time or tracking moving targets precisely. With respect to agility requirements, a control moment gyro (CMG) is a promising actuator to accomplish such a demanding mission.

A CMG is an attitude control actuator that utilizes gyro torque generated by driving a gimbal which has a rotating wheel. A CMG is suitable for a spacecraft that realizes rapid attitude maneuver because of its high torque capability compared to a reaction wheel, which is a common angular momentum exchange actuator. However, there is a problem that the calculation of the optimal attitude maneuver time and trajectory of a spacecraft is complicated when a CMG system is installed.

It is very important for a rapid maneuver to obtain the minimum attitude maneuver time and its trajectory. For example, in an optimal attitude maneuver planning, which optimizes multiple attitude maneuvers of a spacecraft, the minimum attitude maneuver time is used. In the optimal attitude maneuver planning, the minimum attitude maneuver time is required to be calculated in a short time, since it is iterated many times during optimization.

There have been many studies on the trajectory planning of a spacecraft for optimal attitude maneuver, but very few studies use CMGs as actuators. A previous research has shown that the method of solving the time optimization problem of attitude maneuver for a spacecraft to find the minimum attitude maneuver time [1]. Using this method, minimum attitude maneuver time and its trajectory that achieves the exact attitude maneuver can be obtained, but it is difficult to apply it to the optimal attitude maneuver planning because optimization calculations are time consuming. Another study proposed a method to estimate the attitude maneuver time from the maximum angular momentum that a CMG system can output with respect to the rotation axis [2]. With this method, the minimum attitude maneuver time can be calculated in a short time, but it is only applicable to large angle rotations.

In this study, a method is proposed to estimate the minimum attitude maneuver time and its trajectory in a short time when a spacecraft with a CMG system rotates around a given axis at a given angle. In this study, a roof-array system with 90° apex angle, as shown in Fig. 1, is adopted because of the simplicity of the system. This arrangement is a special case of a pyramid-array (skew angle of 90°), also called a 2-SPEED (Two Scis-

sored Pair Ensemble, Explicit Distribution) system.

The remainder of this paper is organized as follows: First, mathematical modeling of the spacecraft motion and the roof-array CMG system is presented in Section 2. In Section 3, the singularity of the roof-array system is discussed and analytical solutions for the maximum angular momentum in any direction are derived. In Section 4, the approximate solution of the minimum attitude maneuver time and its trajectory is described and compared with the result of solving the optimization problem. In Section 5, it is confirmed by the numerical simulations that the desired attitude control is possible by the steering law that follows the reference trajectories obtained by modifying the approximate trajectories. Finally, some conclusions are given in Section 5.

2. Mathematical Modeling of a Spacecraft with CMGs

2.1. Attitude Dynamics

Assuming that the spacecraft and the CMG are rigid bodies, the equation of motion is described as

$$\dot{\boldsymbol{h}} + \boldsymbol{\omega} \times \boldsymbol{h} = \boldsymbol{\tau}_{\text{ext}}, \tag{1}$$

where $\boldsymbol{h}$ is the total angular momentum of the spacecraft, $\boldsymbol{\omega}$ is the angular rate of the spacecraft, and $\boldsymbol{\tau}_{\text{ext}}$ is the disturbance torques input to the spacecraft. The total angular momentum of the spacecraft with the CMG system $\boldsymbol{h}$ can be expressed as follows:

$$\boldsymbol{h} = \boldsymbol{J}\boldsymbol{\omega} + \boldsymbol{h}_{\text{cmg}}, \tag{2}$$

where $\boldsymbol{J}$ is the moment of inertia of the spacecraft, $\boldsymbol{h}_{\text{cmg}}$ is the angular momentum output by the CMG system. Substituting Eq. (2) into Eq. (1), the equation of motion is rewritten as follows:

$$\boldsymbol{J}\dot{\boldsymbol{\omega}} + \dot{\boldsymbol{h}}_{\text{cmg}} + \boldsymbol{\omega} \times \left(\boldsymbol{J}\boldsymbol{\omega} + \boldsymbol{h}_{\text{cmg}}\right) = \boldsymbol{\tau}_{\text{ext}}. \tag{3}$$

2.2. Attitude Kinematics

The attitude of the spacecraft is represented by the quaternion $\boldsymbol{q}$, and the attitude of the spacecraft is expressed as follows:

$$\boldsymbol{q} = \left[\hat{\boldsymbol{\alpha}} \sin\left(\frac{\phi}{2}\right) \;\; \cos\left(\frac{\phi}{2}\right)\right]^{\mathsf{T}}, \tag{4}$$

where $\hat{\boldsymbol{\alpha}} = [\,\alpha_1 \;\; \alpha_2 \;\; \alpha_3\,]^{\mathsf{T}}$ is the unit vector for the rotation axis and ϕ is the rotation angle. The relationship between the quaternion $\boldsymbol{q}$ and the angular rate of the spacecraft $\boldsymbol{\omega}$ is represented by the following differential equation:

$$\dot{\boldsymbol{q}} = \frac{1}{2}\boldsymbol{q} \otimes \boldsymbol{\omega}, \tag{5}$$

where $\otimes$ represents the tensor product defined as

$$\boldsymbol{q}_{\text{A}} \otimes \boldsymbol{q}_{\text{B}} = \begin{bmatrix} 0 & q_{\text{B3}} & -q_{\text{B2}} & q_{\text{B1}} \\ q_{\text{B3}} & 0 & q_{\text{B1}} & q_{\text{B2}} \\ q_{\text{B2}} & -q_{\text{B1}} & 0 & q_{\text{B3}} \\ -q_{\text{B1}} & -q_{\text{B2}} & -q_{\text{B3}} & 0 \end{bmatrix} \boldsymbol{q}_{\text{A}}. \tag{6}$$

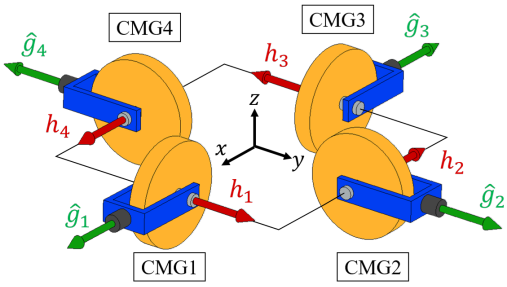

Fig. 1. Roof array CMG model

2.3. Roof-Array CMG System

The angular momentum of the roof-array CMG system $\boldsymbol{h}_{\text{cmg}}$ is expressed as the sum of the angular momentum of each CMG $\boldsymbol{h}_i$ as

$$\begin{aligned} \boldsymbol{h}_{\text{cmg}}(\boldsymbol{\theta}) &= \boldsymbol{h}_1(\theta_1) + \boldsymbol{h}_2(\theta_2) + \boldsymbol{h}_3(\theta_3) + \boldsymbol{h}_4(\theta_4), \\ &= h_{\text{w}} \begin{bmatrix} -\cos\theta_2 + \cos\theta_4 \\ \cos\theta_1 - \cos\theta_3 \\ \sin\theta_1 + \sin\theta_2 + \sin\theta_3 + \sin\theta_4 \end{bmatrix}, \end{aligned} \tag{7}$$

where h_{w} denotes the magnitude of the angular momentum of each CMG and $\boldsymbol{\theta} = [\theta_1 \;\; \theta_2 \;\; \theta_3 \;\; \theta_4]^{\mathsf{T}}$ is a matrix of the gimbal angles. From Eq. (7), the torque applied to the spacecraft by the roof-array CMG system $\boldsymbol{\tau}_{\text{cmg}}$ is expressed as

$$\boldsymbol{\tau}_{\text{cmg}}(\dot{\boldsymbol{\theta}}) = -\dot{\boldsymbol{h}}_{\text{cmg}} = -\sum_{i=1}^{4} \frac{\partial \boldsymbol{h}_i}{\partial \theta_i}\dot{\theta}_i = -h_{\text{w}}\boldsymbol{A}\dot{\boldsymbol{\theta}}, \tag{8}$$

where $\boldsymbol{A}$ is the matrix represented by

$$\boldsymbol{A} = \begin{bmatrix} 0 & \sin\theta_2 & 0 & -\sin\theta_4 \\ -\sin\theta_1 & 0 & \sin\theta_3 & 0 \\ \cos\theta_1 & \cos\theta_2 & \cos\theta_3 & \cos\theta_4 \end{bmatrix}. \tag{9}$$

Depending on the combination of gimbal angles, $\boldsymbol{A}$ may not be full rank. In this case, according to Eq. (8), the torque cannot be output in a certain direction. Such a problem is called the singularity problem.

3. Singular State Analysis of the Roof-Type CMGs

In this section, the angular momentum in a singular state of the roof-array system is considered. Furthermore, the analytical solutions for the maximum angular momentum for any direction are derived.

3.1. Angular Momentum in a Singular State

When the CMG system is in a singular state, it satisfies the following equation:

$$\det(\boldsymbol{A}\boldsymbol{A}^{\mathsf{T}}) = 0. \tag{10}$$

Using the Binet-Cauchy theorem, Eq. (10) can be expressed as follows [3]:

$$\det(\boldsymbol{A}\boldsymbol{A}^{\mathsf{T}}) = \sum_{i=1}^{4} \det(\boldsymbol{A}_i)^2, \tag{11}$$

where $\boldsymbol{A}_i$ is a matrix with the *i-th* column of $\boldsymbol{A}$ removed. By computing Eq. (10) with the relationship in Eq. (11), the following equation is obtained.

$$(\sin\theta_1\sin(\theta_2+\theta_4))^2+(\sin\theta_2\sin(\theta_1+\theta_3))^2 + (\sin\theta_3\sin(\theta_2+\theta_4))^2+(\sin\theta_4\sin(\theta_1+\theta_3))^2=0. \tag{12}$$

From Eq. (12), in a singular state, the gimbal angles satisfy the following equations:

$$\begin{cases} \sin(\theta_1+\theta_3),\ \sin(\theta_2+\theta_4)=0, \\ \sin(\theta_1+\theta_3),\ \sin\theta_1,\ \sin\theta_3=0, \\ \sin(\theta_2+\theta_4),\ \sin\theta_2,\ \sin\theta_4=0, \\ \sin\theta_1,\ \sin\theta_2,\ \sin\theta_3,\ \sin\theta_4=0. \end{cases} \tag{13}$$

For each case, the angular momentums of the CMG system in a singular state are obtained as follows:

$$\boldsymbol{h}_{\mathrm{cmg}} = h_{\mathrm{w}}\begin{bmatrix} -2\cos\theta_2 \\ 2\cos\theta_1 \\ 2\sin\theta_1+2\sin\theta_2 \end{bmatrix}, \tag{14}$$

$$\boldsymbol{h}_{\mathrm{cmg}} = h_{\mathrm{w}}\begin{bmatrix} -\cos\theta_2+\cos\theta_4 \\ 0,\pm2 \\ \sin\theta_2+\sin\theta_4 \end{bmatrix}, \tag{15}$$

$$\boldsymbol{h}_{\mathrm{cmg}} = h_{\mathrm{w}}\begin{bmatrix} 0,\pm2 \\ \cos\theta_1-\cos\theta_3 \\ \sin\theta_1+\sin\theta_3 \end{bmatrix}. \tag{16}$$

These are illustrated in Fig. 2, with the magnitude of the angular momentum of each CMG as $h_{\mathrm{w}}=1$.

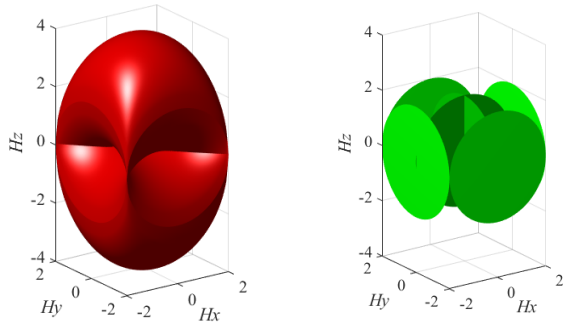

(a) Eq. (14) (b) Eqs. (15) and (16)

Fig. 2. Angular momentum of the roof-array system in a singular state

3.2. External 2H Singular State

1. When the angular momentum in the x direction is $\pm2h_{\mathrm{w}}$ (Eq. (16))

   In the 2H singular surface, when the angular momentum in the x direction is $\pm2h_{\mathrm{w}}$, it constitutes an angular momentum envelope. With $\theta_p=\frac{\theta_1+\theta_3}{2}$ and $\theta_m=\frac{\theta_1-\theta_3}{2}$, Eq. (16) is rewritten as follows:

   $$\boldsymbol{h}_{\mathrm{cmg}} = 2h_{\mathrm{w}}\begin{bmatrix} \pm1 \\ -\sin\theta_p\sin\theta_m \\ \sin\theta_p\cos\theta_m \end{bmatrix}. \tag{17}$$

   Let $\hat{\boldsymbol{h}}=[\ \hat{h}_1\ \ \hat{h}_2\ \ \hat{h}_3\ ]^{\mathrm{T}}$ be the unit vector of the angular momentum direction of the CMG system, then the following equation is satisfied from Eq. (17):

   $$\hat{\boldsymbol{h}} = \frac{1}{\sqrt{1+\sin^2\theta_p}}\begin{bmatrix} \pm1 \\ -\sin\theta_p\sin\theta_m \\ \sin\theta_p\cos\theta_m \end{bmatrix}. \tag{18}$$

   From Eq. (18), the following inequality is satisfied:

   $$\hat{h}_2^2+\hat{h}_3^2\le\hat{h}_1^2, \tag{19}$$

   $$\Leftrightarrow\quad \hat{h}_1^2\ge\frac{1}{2}. \tag{20}$$

   From Eqs. (17) and (18), the magnitude of the maximum angular momentum in this case is expressed as

   $$\|\boldsymbol{h}_{\mathrm{cmg}}\| = \frac{2h_{\mathrm{w}}}{|\hat{h}_1|}. \tag{21}$$

2. When the angular momentum in the y direction is $\pm2h_{\mathrm{w}}$ (Eq. (15))

   Similarly, when the unit vector of angular momentum satisfies the following inequality:

   $$\hat{h}_2^2\ge\frac{1}{2}, \tag{22}$$

   the magnitude of the maximum angular momentum is expressed as

   $$\|\boldsymbol{h}_{\mathrm{cmg}}\| = \frac{2h_{\mathrm{w}}}{|\hat{h}_2|}. \tag{23}$$

3.3. 4H Singular State

Angular momentum envelope consists of the 4H singular state except for the 2H singular state. Therefore, the condition in this case is expressed in the following inequality:

$$\hat{h}_1^2,\ \hat{h}_2^2<\frac{1}{2}. \tag{24}$$

In the case of the 4H singular state, Eq. (14) holds under the following equation:

$$\theta_1+\theta_3=\pi,\quad \theta_2+\theta_4=\pi. \tag{25}$$

From Eq. (14), the following equation holds for the unit vector $\hat{\boldsymbol{h}}$:

$$\hat{\boldsymbol{h}} = \frac{1}{\sqrt{2\,(1+\sin\theta_1\sin\theta_2)}}\begin{bmatrix} -\cos\theta_2 \\ \cos\theta_1 \\ \sin\theta_1+\sin\theta_2 \end{bmatrix}. \tag{26}$$

From the 1, 2 components in Eq. (26) with $x=\sin\theta_1$ and $y=\sin\theta_2$, the following equations are obtained for x, y:

$$\begin{aligned} 1-y^2-2\hat{h}_1^2\,(1+xy)=0, \\ 1-x^2-2\hat{h}_2^2\,(1+xy)=0. \end{aligned} \tag{27}$$

There are four solutions for x, y in these equations as

$$x=\pm1,\ y=\mp1,\quad x=\pm\frac{1-2\hat{h}_2^2}{\sqrt{1-4\hat{h}_1^2\hat{h}_2^2}},\ y=\pm\frac{1-2\hat{h}_1^2}{\sqrt{1-4\hat{h}_1^2\hat{h}_2^2}}. \quad \text{(double-sign corresponds)} \tag{28}$$

Of these, the cases of $x=\pm1$, $y=\mp1$ do not results in the 4H singular state because $\hat{h}_3=0$. From Eqs. (14), (26), and (28), the magnitude of the maximum angular momentum is expressed in the following equation:

$$\|\boldsymbol{h}_{\mathrm{cmg}}\| = \frac{4h_{\mathrm{w}}|\hat{h}_3|}{\sqrt{1-4\hat{h}_1^2\hat{h}_2^2}}. \tag{29}$$

3.4. Summary of Angular Momentum Envelope

The magnitude of the maximum angular momentum that the roof-array CMG system has in a given unit vector direction $\hat{\boldsymbol{h}}$ is summarized in Table 1. Each component of the unit vector $\hat{\boldsymbol{h}}$ is as follows:

$$\hat{\boldsymbol{h}} = \begin{bmatrix} \hat{h}_1 \\ \hat{h}_2 \\ \hat{h}_3 \end{bmatrix}, \quad \hat{h}_1^2 + \hat{h}_2^2 + \hat{h}_3^2 = 1.$$

Table 1. The maximum angular momentum at any direction

Conditions	Type	Magnitude
$\lvert\hat{h}_1\rvert \geq \sqrt{2}/2$	2H	$2h_w/\lvert\hat{h}_1\rvert$
$\lvert\hat{h}_2\rvert \geq \sqrt{2}/2$	2H	$2h_w/\lvert\hat{h}_2\rvert$
$\lvert\hat{h}_1\rvert,\ \lvert\hat{h}_2\rvert < \sqrt{2}/2$	4H	$4h_w\lvert\hat{h}_3\rvert/\sqrt{1-4\hat{h}_1^2\hat{h}_2^2}$

4. Approximate Solution of Time-Optimal Maneuver

In this section, a method for estimating the minimum attitude maneuver time and its trajectory of the spacecraft with the CMG system is proposed.

4.1. Estimation of Maneuver Time

Consider a rest-to-rest maneuver in which the spacecraft rotates at an angle $\phi_f \in [0, \pi]$ around an arbitrary unit vector $\hat{\boldsymbol{\alpha}}$. The rate trajectory of the spacecraft around $\hat{\boldsymbol{\alpha}}$ in this case is shown in Fig. 3. First, it accelerates from the initial state for a gimbal drive time T_{gimbal}, and then, rotates at a constant speed ω_c around $\hat{\boldsymbol{\alpha}}$ for a constant gimbal angle time T_c. Finally, the attitude change is completed by decelerating for gimbal drive time T_{gimbal}.

Assuming that the initial and final states of the gimbal angle are the same, the gimbal drive time during deceleration is considered to be the same with that during acceleration. Therefore, using T_{gimbal} and T_c, the attitude maneuver time of the spacecraft T is expressed as follows:

$$T = 2T_{\text{gimbal}} + T_c. \tag{30}$$

By approximating the rotation angle of the spacecraft during T_{gimbal} to $\omega_c T_{\text{gimbal}}/2$ around the $\hat{\boldsymbol{\alpha}}$ axis, the gimbal angle constant time T_c can be estimated as

$$T_c = \frac{\left(\phi_f - \omega_c T_{\text{gimbal}}\right)}{\omega_c} \qquad \left(\phi_f \geq \omega_c T_{\text{gimbal}}\right). \tag{31}$$

Suppose that the CMG system outputs an angular momentum of arbitrary magnitude h_{mag} in the $-J\hat{\boldsymbol{\alpha}}$ direction during T_c in order for the spacecraft to rotate around $\hat{\boldsymbol{\alpha}}$. The spacecraft rate ω_c around $\hat{\boldsymbol{\alpha}}$ during T_c is as follows from Eq. (2):

$$\begin{aligned} \boldsymbol{J\omega_c} &= \frac{\boldsymbol{J\hat{\alpha}}}{\|\boldsymbol{J\hat{\alpha}}\|} h_{\text{mag}}, \\ \Leftrightarrow \quad \boldsymbol{\omega_c} &= \frac{h_{\text{mag}}}{\|\boldsymbol{J\hat{\alpha}}\|}\hat{\boldsymbol{\alpha}}, \\ \Leftrightarrow \quad \omega_c &= \frac{h_{\text{mag}}}{\|\boldsymbol{J\hat{\alpha}}\|}. \end{aligned} \tag{32}$$

From Eqs. (30), (31), and (32), the attitude maneuver time T can be estimated as follows:

$$\begin{aligned} &h_{\text{mag}} \leq \frac{\|\boldsymbol{J\hat{\alpha}}\|}{T_{\text{gimbal}}}\phi_f : && T = T_{\text{gimbal}} + \frac{\|\boldsymbol{J\hat{\alpha}}\|}{h_{\text{mag}}}\phi_f, \\ &h_{\text{mag}} > \frac{\|\boldsymbol{J\hat{\alpha}}\|}{T_{\text{gimbal}}}\phi_f : && T \text{ cannot be computed because } h_{\text{mag}} \text{ is too large.} \end{aligned} \tag{33}$$

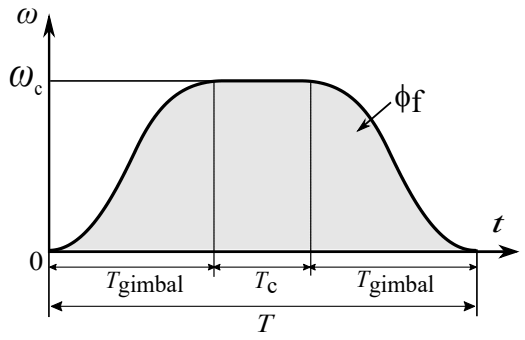

Fig. 3. The rate trajectory of the spacecraft around $\hat{\boldsymbol{\alpha}}$

4.2. Derivation of Minimum Gimbal Drive Time

Given the gimbal angle $\boldsymbol{\theta}_c$ which outputs the angular momentum of magnitude h_{mag} in the $-\boldsymbol{J\hat{\alpha}}$ direction, the gimbal angle reaches $\boldsymbol{\theta}_c$ from its initial state $\boldsymbol{\theta}_0$ during the gimbal drive time T_{gimbal}. The maximum values of gimbal rate and gimbal angular acceleration are set to $\dot{\theta}_{\max}$ and $\ddot{\theta}_{\max}$, respectively, and the gimbal rate trajectories for the minimum drive time are shown in Fig. 4. From Fig. 4, the gimbal angle displacement is expressed as

$$\|\boldsymbol{\theta}_c - \boldsymbol{\theta}_0\|_\infty = \begin{cases} \dfrac{\ddot{\theta}_{\max} T_{\text{gimbal}}^2}{4} & \left(T_{\text{gimbal}} < \dfrac{2\dot{\theta}_{\max}}{\ddot{\theta}_{\max}}\right), \\ \dot{\theta}_{\max} T_{\text{gimbal}} - \dfrac{\dot{\theta}_{\max}^2}{\ddot{\theta}_{\max}} & \left(T_{\text{gimbal}} \geq \dfrac{2\dot{\theta}_{\max}}{\ddot{\theta}_{\max}}\right). \end{cases} \tag{34}$$

Therefore, the minimum gimbal drive time is represented as follows:

$$T_{\text{gimbal}} = \begin{cases} 2\sqrt{\dfrac{\|\boldsymbol{\theta}_c - \boldsymbol{\theta}_0\|_\infty}{\ddot{\theta}_{\max}}} & \left(T_{\text{gimbal}} < \dfrac{2\dot{\theta}_{\max}}{\ddot{\theta}_{\max}}\right), \\ \dfrac{\|\boldsymbol{\theta}_c - \boldsymbol{\theta}_0\|_\infty}{\dot{\theta}_{\max}} + \dfrac{\dot{\theta}_{\max}}{\ddot{\theta}_{\max}} & \left(T_{\text{gimbal}} \geq \dfrac{2\dot{\theta}_{\max}}{\ddot{\theta}_{\max}}\right). \end{cases} \tag{35}$$

As can be seen from the above equation, it is necessary to choose $\boldsymbol{\theta}_c$ that satisfies the following equation to minimize T_{gimbal}:

$$\text{minimize} \ \ \|\boldsymbol{\theta}_c - \boldsymbol{\theta}_0\|_\infty. \tag{36}$$

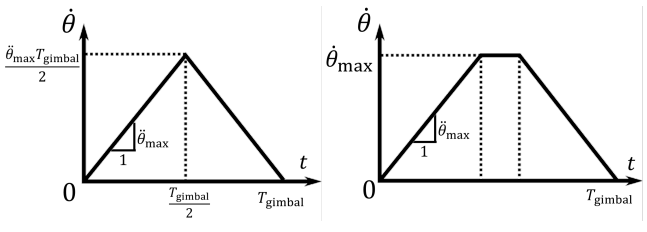

(a) Triangular trajectory (b) Trapezoidal trajectory

Fig. 4. The gimbal rate trajectory

4.3. Calculation of Gimbal Angle

A method to find the gimbal angle that outputs an arbitrary angular momentum $\boldsymbol{h}_{\mathrm{cmg}}$ inside the angular momentum envelope is described. First, the angular momentum of the CMG system is divided by h_{w} and denoted as

$$\boldsymbol{h}_0 = \frac{\boldsymbol{h}_{\mathrm{cmg}}}{h_{\mathrm{w}}} = \begin{bmatrix} h_{10} \\ h_{20} \\ h_{30} \end{bmatrix}. \tag{37}$$

In this case, the following equations hold from Eq. (7),

$$\begin{aligned} -c_2 + c_4 &= h_{10}, \\ c_1 - c_3 &= h_{20}, \\ s_1 + s_2 + s_3 + s_4 &= h_{30}. \end{aligned} \tag{38}$$

Since there are four CMGs, there are generally innumerable solutions that satisfy the above equations. Therefore, given a value of a gimbal angle, calculate the values of the three remaining gimbal angles. In this case, the value of θ_4 is given as

$$\begin{aligned} -c_2 = h_{10} - c_4 &= h_1, \\ c_1 - c_3 &= h_{20} = h_2, \\ s_1 + s_2 + s_3 &= h_{30} - s_4 = h_3. \end{aligned} \tag{39}$$

The solution is obtained by solving the above equations and the following equations for trigonometric functions:

$$s_1^2 + c_1^2 = 1, \quad s_2^2 + c_2^2 = 1, \quad s_3^2 + c_3^2 = 1. \tag{40}$$

First, from Eq. (39), c_2 and s_2 are given as

$$c_2 = -h_1, \quad s_2 = \pm\sqrt{1 - c_2^2}. \tag{41}$$

From the Gröbner basis, the quadratic equation for s_1 is obtained as

$$s_1^2 + (h_3 - s_2)\, s_1 + \frac{h_2^2 + (h_3 - s_2)^2}{4} - \frac{h_2^2}{h_2^2 + (h_3 - s_2)^2} = 0. \tag{42}$$

This equation is solved in the following cases:

1. $h_2 \neq 0$
   The discriminant D in Eq. (42) is expressed as

$$D = h_2^2 \left(\frac{4}{h_2^2 + (h_3 - s_2)^2} - 1 \right). \tag{43}$$

   If $D < 0$, the solution is not obtained for a given θ_4. If $D \geq 0$, s_1 is given as follows:

$$s_1 = \frac{h_3 - s_2}{2} \pm \frac{\sqrt{D}}{2}. \tag{44}$$

   In addition, c_1 is given as

$$c_1 = \frac{h_2^2 + (h_3 - s_2)^2 - 2 s_1 (h_3 - s_2)}{2 h_2}. \tag{45}$$

   Further, c_3 and s_3 are given as

$$\begin{aligned} c_3 &= \frac{-h_2^2 + (h_3 - s_2)^2 - 2 s_1 (h_3 - s_2)}{2 h_2}, \\ s_3 &= h_3 - s_1 - s_2. \end{aligned} \tag{46}$$

2. $h_2 = 0$
   The solution for $h_2 = 0$ is given as follows:

$$\begin{aligned} c_2 = -h_1, \; s_2 &= \pm\sqrt{1 - c_2^2}, \\ s_1 = \frac{h_3 - s_2}{2}, \; c_1 &= \pm\sqrt{1 - s_1^2}, \\ \theta_3 &= \theta_1. \end{aligned} \tag{47}$$

These enable the solutions θ_1, θ_2, and θ_3 to be found. In this study, θ_4 is divided into 100 equal parts in the $[-\pi, \pi]$ region and the solutions are obtained for each of the given θ_4. Among the obtained gimbal angles, the one satisfying Eq. (36) is used as the solution for the gimbal angle.

4.4. Minimum Time Attitude Maneuver Trajectory

The gimbal angle and rate trajectories of CMGs are described. First, the gimbal angle is driven from initial state of $\boldsymbol{\theta}_0$ to $\boldsymbol{\theta}_{\mathrm{c}}$ during T_{gimbal}. The gimbal rate trajectory during T_{gimbal} is classified according to whether the gimbal rate reaches the upper limit or not as follows:

1. Triangle Trajectory ($\left|\theta_{\mathrm{c},i} - \theta_{0,i}\right| \leq T_{\mathrm{gimbal}} \dot{\theta}_{\max}/2$)
   The gimbal angular acceleration a_i of the *i-th* CMG is represented by

$$a_i = \frac{4\left(\theta_{\mathrm{c},i} - \theta_{0,i}\right)}{T_{\mathrm{gimbal}}^2}. \tag{48}$$

   Then, the gimbal rate trajectory is given as follows:

$$\dot{\theta}_i(t) = \begin{cases} a_i t & \left(0 \leq t \leq \frac{T_{\mathrm{gimbal}}}{2}\right), \\ -a_i \left(t - T_{\mathrm{gimbal}}\right) & \left(\frac{T_{\mathrm{gimbal}}}{2} < t \leq T_{\mathrm{gimbal}}\right). \end{cases} \tag{49}$$

2. Trapezoidal Trajectory ($\left|\theta_{\mathrm{c},i} - \theta_{0,i}\right| > T_{\mathrm{gimbal}} \dot{\theta}_{\max}/2$)
   The gimbal angle acceleration time $t_{\mathrm{acc},i}$, the gimbal angle constant time $t_{\mathrm{c},i}$ and the gimbal angular acceleration a_i of the *i th* CMG is represented by

$$\begin{aligned} t_{\mathrm{c},i} &= \frac{2\left|\theta_{\mathrm{c},i} - \theta_{0,i}\right|}{\dot{\theta}_{\max}} - T_{\mathrm{gimbal}}, \\ t_{\mathrm{acc},i} &= \frac{\left(T_{\mathrm{gimbal}} - t_{\mathrm{c},i}\right)}{2}, \\ a_i &= \pm\frac{\dot{\theta}_{\max}}{t_{\mathrm{acc},i}}. \end{aligned} \tag{50}$$

   Then, the gimbal rate trajectory is given as follows:

$$\dot{\theta}_i(t) = \begin{cases} a_i t & \left(0 \leq t \leq t_{\mathrm{acc},i}\right), \\ \pm\dot{\theta}_{\max} & \left(t_{\mathrm{acc},i} < t \leq t_{\mathrm{acc},i} + t_{\mathrm{c},i}\right), \\ -a_i \left(t - T_{\mathrm{gimbal}}\right) & \left(t_{\mathrm{acc},i} + t_{\mathrm{c},i} < t \leq T_{\mathrm{gimbal}}\right). \end{cases} \tag{51}$$

After the gimbal angle reaches $\boldsymbol{\theta}_{\mathrm{c}}$, the gimbal angle keeps $\boldsymbol{\theta}_{\mathrm{c}}$ during T_{c}. After T_{c}, the gimbal angle and rate trajectories track the same trajectories in the acceleration.

The rate trajectory of the spacecraft $\boldsymbol{\omega}(t)$ is obtained from Eq. (2), assuming that the total angular momentum of the spacecraft is $\mathbf{0}$,

$$\boldsymbol{\omega}(t) = -\boldsymbol{J}^{-1} \boldsymbol{h}_{\mathrm{cmg}}(\boldsymbol{\theta}(t)). \tag{52}$$

The attitude trajectory of the spacecraft is obtained from Eq. (5).

4.5. Overview of Estimation Method

An overview of the minimum attitude maneuver time and its trajectory estimation is shown in Fig. 5. First, find the maximum angular momentum in the $-J\hat{\boldsymbol{\alpha}}$ direction. Then, give the CMG system an angular momentum of arbitrary magnitude $h_{\mathrm{mag}} \in [0,\ h_{\mathrm{env}}]$ and compute the gimbal angle that outputs it. Then, the gimbal drive time T_{gimbal} is calculated, and the attitude maneuver time T is obtained. The minimum attitude maneuver time is determined by searching for h_{mag} that minimizes the attitude maneuver time T by a golden split search.

In the case of an actual attitude control, the approximation of the trajectory is made according to Fig. 5.

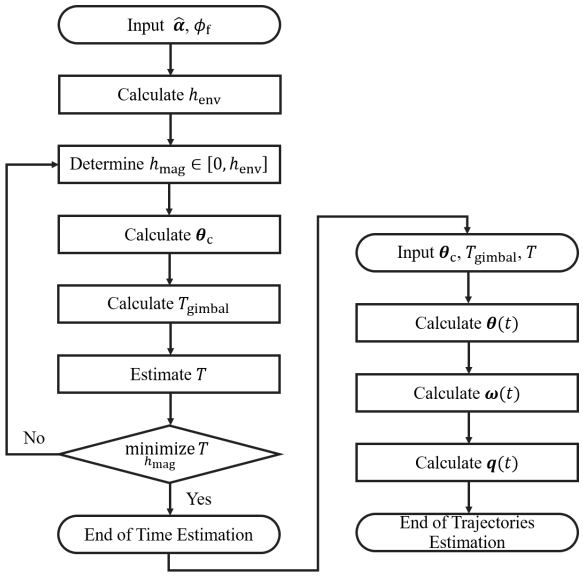

Fig. 5. An overview of the estimation method

4.6. Minimum Attitude Maneuver Time in All Directions

The minimum attitude maneuver time obtained by the proposed method is compared with the optimal time obtained using a nonlinear optimization program for the minimum attitude maneuver time. The minimum attitude maneuver time is compared for a rotation axis in all directions in the case of the rotation angle fixed at $\phi_{\mathrm{f}} = 5, 10, 30, 60$.

Figure 6 shows a view of the illustration of the minimum attitude maneuver time in all directions. When drawing the axis from the origin to the envelope, the direction of the axis indicates the direction of the rotation axis $\hat{\boldsymbol{\alpha}}$, and its length represents the minimum attitude maneuver time T in that direction. The parameter values are listed in Table 2. The approximate

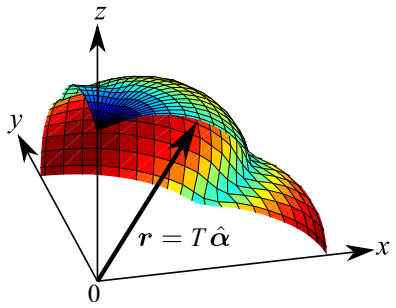

Fig. 6. A view of an illustration of minimum attitude maneuver time in all directions

maneuver times and the minimum maneuver times obtained using a nonlinear optimization program are shown in Fig.7, and

Table 2. Parameter values

parameter	value
$\boldsymbol{J}$ [kgm^2]	diag[1 1.2 1.5]
h_{w} [Nms]	0.05
$\dot{\theta}_{\mathrm{max}}$ [rad/s]	1
$\ddot{\theta}_{\mathrm{max}}$ [rad/s^2]	2
$\boldsymbol{\theta}_0$ [deg]	$[30, -30, 30, -30]^{\mathsf{T}}$

their average are listed in Table 3. The approximate values were used as the initial values of the optimal calculation.

From, Fig. 7, it can be confirmed that the approximate results capture the characteristics of the optimization results in all directions. From, Table 3, The average time differences are less than a few percent and the deviations are also small.

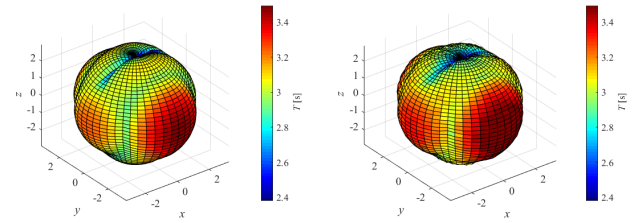

(a) $\phi_{\mathrm{f}} = 5$ deg

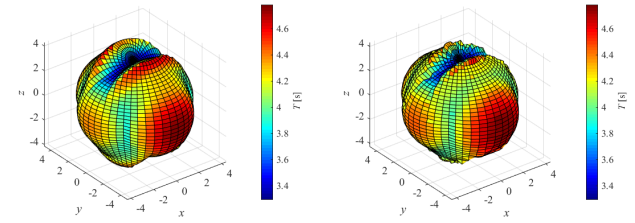

(b) $\phi_{\mathrm{f}} = 10$ deg

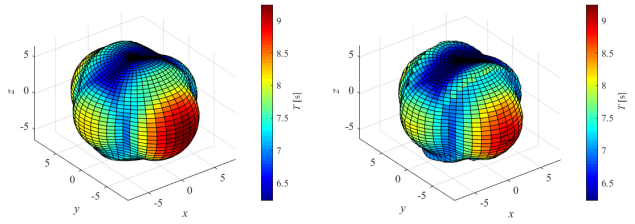

(c) $\phi_{\mathrm{f}} = 30$ deg

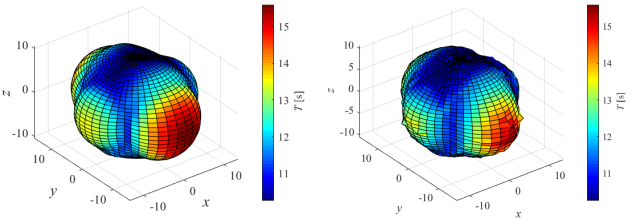

(d) $\phi_{\mathrm{f}} = 60$ deg

Fig. 7. The illustrations of the minimum attitude maneuver time in all directions, left : approximate solutions, right : optimal solutions

Table 4 shows the results of the average computation time per direction when calculating the attitude maneuver time in all directions. The computation times are found to be significantly reduced. Furthermore, the computation times for the approximate method are almost the same at different rotation angles, while the computation times for the optimization method vary

Table 3. Comparison of optimal and approximate maneuver time

ϕ_f [deg]	Approximate Average [s]	Optimal Average [s]	Optimal/Approximate		
			Ave	Max	Min
5	3.01	3.03	1.01	1.05	0.94
10	4.05	4.08	1.01	1.11	0.91
30	7.22	6.99	0.97	1.06	0.89
60	11.7	11.4	0.97	1.08	0.91

significantly. This is because the initial value has a great effect on the computation time in the optimization method.

Table 4. Comparison of average calculation time (i7-6700 CPU)

ϕ_f [deg]	Approximate [s]	Optimal [s]
5	2.75×10^{-3}	4.80
10	2.42×10^{-3}	5.43
30	1.88×10^{-3}	8.56
60	2.25×10^{-3}	12.6

5. Attitude Control Simulation

5.1. Overview of Attitude Control

An overview of the attitude control laws for the spacecraft is shown in Fig. 8. In the case of an actual attitude control, an approximation of the trajectory is generated after an approximation of the attitude maneuver time. After generating the trajectory, that is modified by the interior point method to reach the target attitude exactly. The modified gimbal rate trajectory and the attitude and rate trajectories of the spacecraft are used as the reference trajectories. The control and steering laws provide the feedback attitude control to follow their reference trajectories.

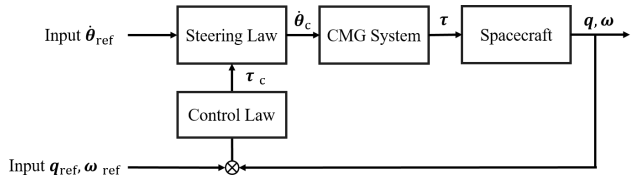

Fig. 8. Attitude Control law

5.2. Attitude Control and Steering Law

A control law is constructed to follow the generated reference attitude and rate trajectories of the spacecraft. The control torque $\boldsymbol{\tau}_{\mathrm{c}}$ is defined by the PD feedback control as

$$\begin{aligned} \boldsymbol{q}_{\mathrm{e}} &= \boldsymbol{q} \otimes \boldsymbol{q}_{\mathrm{ref}}^{\dagger}, \quad \boldsymbol{\omega}_{\mathrm{e}} = \boldsymbol{\omega} - \boldsymbol{\omega}_{\mathrm{ref}}, \\ \boldsymbol{\tau}_{\mathrm{c}} &= k_{\mathrm{p}} V(\boldsymbol{q}_{\mathrm{e}}) + k_{\mathrm{d}} \boldsymbol{\omega}_{\mathrm{e}}, \end{aligned} \tag{53}$$

where $V(\boldsymbol{q}_{\mathrm{e}})$ is the vector part of $\boldsymbol{q}_{\mathrm{e}}$ and $\boldsymbol{q}_{\mathrm{ref}}^{\dagger}$ is conjugate quaternion of $\boldsymbol{q}_{\mathrm{ref}}$.

In this study, a steering law that modifies the gimbal rate by the feedback is adopted for the reference gimbal rate trajectory $\dot{\boldsymbol{\theta}}_{\mathrm{ref}}$.

$$\dot{\boldsymbol{\theta}}_{\mathrm{c}} = \dot{\boldsymbol{\theta}}_{\mathrm{ref}} - \frac{1}{h_{\mathrm{w}}} \boldsymbol{A}^{\#} \boldsymbol{\tau}_{\mathrm{c}}, \tag{54}$$

where $\boldsymbol{A}^{\#}$ is defined as follows:

$$\boldsymbol{A}^{\#} = \boldsymbol{A}^{\mathsf{T}} \frac{\mathrm{adj}\left(\boldsymbol{A}\boldsymbol{A}^{\mathsf{T}}\right)}{\max\left(\det\left(\boldsymbol{A}\boldsymbol{A}^{\mathsf{T}}\right), \epsilon\right)}, \tag{55}$$

where adj represents cofactor matrix. In order to investigate the characteristics of this steering law, $\boldsymbol{A}$ is decomposed into the following, with $\sigma_1 \geq \sigma_2 \geq \sigma_3$:

$$\boldsymbol{A} = \boldsymbol{U} \begin{bmatrix} \sigma_1 & 0 & 0 & 0 \\ 0 & \sigma_2 & 0 & 0 \\ 0 & 0 & \sigma_3 & 0 \end{bmatrix} \boldsymbol{V}^{\mathsf{T}}. \tag{56}$$

Thereby, Eq. (55) is rewritten as follows:

$$\boldsymbol{A}^{\#} = \frac{1}{\max\left(\det\left(\boldsymbol{A}\boldsymbol{A}^{\mathsf{T}}\right), \epsilon\right)} \boldsymbol{V} \begin{bmatrix} \sigma_1\sigma_2^2\sigma_3^2 & 0 & 0 \\ 0 & \sigma_1^2\sigma_2\sigma_3^2 & 0 \\ 0 & 0 & \sigma_1^2\sigma_2^2\sigma_3 \\ 0 & 0 & 0 \end{bmatrix} \boldsymbol{U}^{\mathsf{T}}, \tag{57}$$

where ϵ is a positive scalar that prevents $\boldsymbol{A}^{\#}$ from diverging. As the CMG system approaches the singular state, $\sigma_3 = 0$, ie. $\boldsymbol{A}^{\#} = \boldsymbol{0}$, the feedforward term is dominant in Eq. (54). Therefore, the feedback control is effective far from the singular state, and the feedforward control is dominant near the singular state.

5.3. Numerical Simulation Results

In this subsection, as an example, a simulation of attitude control for the 30 degree rotation around the rotation axis $[0 \ \ 0 \ \ 1]^{\mathsf{T}}$ is performed. The initial state of the gimbal angle was chosen to be $[30, -30, 30, -30]^{\mathsf{T}}$ degree as an example of a state with zero angular momentum and a non-singular state. The parameter values used in the simulation are listed in Table 5.

Table 5. Parameter values in attitude control simulation

parameter	value
$\boldsymbol{J}$ [kgm^2]	diag[0.66 0.66 1]
h_{w} [Nms]	0.0576
k_{p} [Nm]	5
k_{d} [Nms/rad]	5
$\dot{\theta}_{\max}$ [rad/s]	4
$\ddot{\theta}_{\max}$ [rad/s^2]	4
$\boldsymbol{\theta}_0$ [deg]	$[30, -30, 30, -30]^{\mathsf{T}}$
$\hat{\boldsymbol{\alpha}}$	$[0 \ \ 0 \ \ 1]^{\mathsf{T}}$
ϕ_f [deg]	30

The actual inertia matrix $\boldsymbol{J}_{\mathrm{r}}$ is given by

$$\boldsymbol{J}_{\mathrm{r}} = \boldsymbol{J} + \begin{bmatrix} 0.03 & 0.01 & 0.02 \\ 0.01 & 0.03 & 0.01 \\ 0.02 & 0.01 & 0.03 \end{bmatrix} \ \mathrm{kgm}^2. \tag{58}$$

The approximate trajectories and the modified trajectories are shown in Fig. 9. The approximate trajectories can be modified by the interior point method to create the reference trajectories that arrive at an exact target orientation.

The results of the attitude control simulation are shown in Fig. 10. From Fig. 10 (d), it can be seen that the CMG system falls into a singular state around 1 to 2 seconds. However, gimbal angle is not significantly affected by the singular state, as shown in Fig. 10 (a). As shown in Fig. 10 (b) and (c), the spacecraft is able to follow its reference trajectory without any

fluctuation in its attitude, even though it is temporarily in the singular state. This is one of the advantages of the proposed method of creating the FF gimbal rate trajectory.

6. Conclusion

In this study, an approximate solution of the minimum attitude maneuver time and its attitude trajectory for a rest-to-rest maneuver of the spacecraft with the roof-array CMG system is derived. In calculating the approximate solution, the analytical solutions for the maximum angular momentum of the roof-array CMG system in any direction by using inverse kinematics and approximating the attitude maneuver of the spacecraft are used to reduce the computational cost. The obtained approximate minimum attitude maneuver times are used to accurately estimate the optimal solutions. Using numerical simulations, it has been demonstrated that the attitude control is possible by following the reference trajectories that are the modified approximate trajectories.

References

1) H. Kobayashi et al., Optimal Attitude Maneuver Plan for Spacecraft with Pyramid-type CMGs Using the Pseudo-Spectral Method, *The Japan Society for Aeronautical and Space Sciences*, **16** (2017), pp. 55-63 (in Japanese).
2) S. Kawajiri et al., A Low-complexity Attitude Control Method for Large-angle Agile Maneuvers of a Spacecraft with Control Moment Gyros, *Acta Astronautica*, **139** (2017), pp. 486-493.
3) B. Wie et al., Singularity Analysis and Visualization for Single-Gimbal Control Moment Gyro Systems, *J. Guid. Control Dyn. 27*, **2** (2004), pp. 271–282.

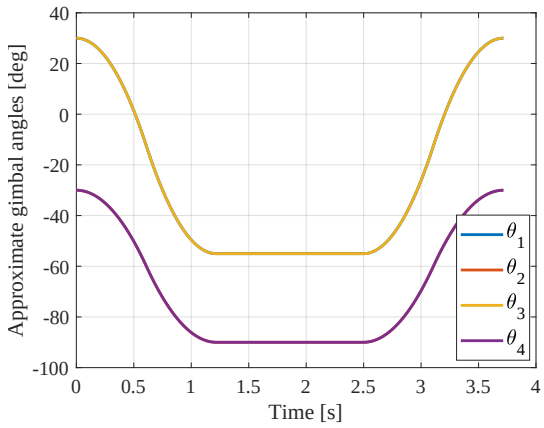

(a) Approximate gimbal angles

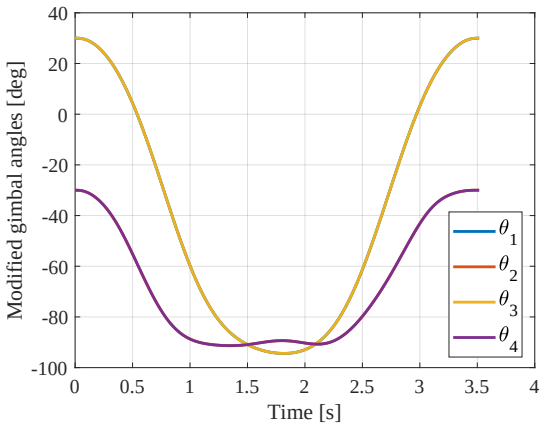

(a) Modified gimbal angles

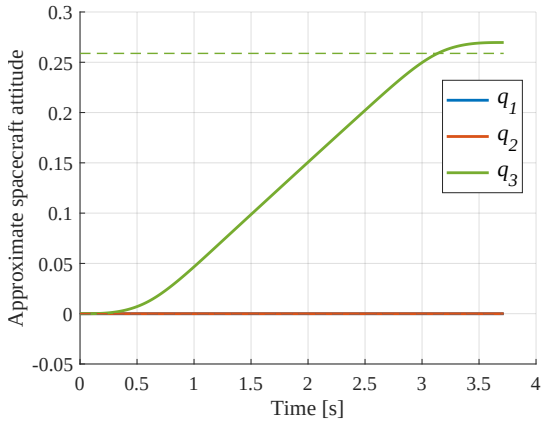

(a) Approximate attitude of the spacecraft

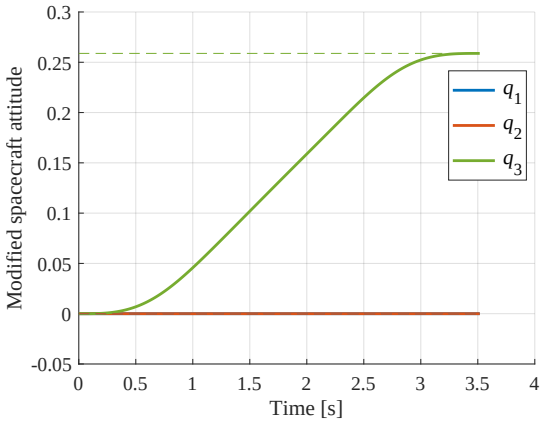

(b) Modified attitude of the spacecraft

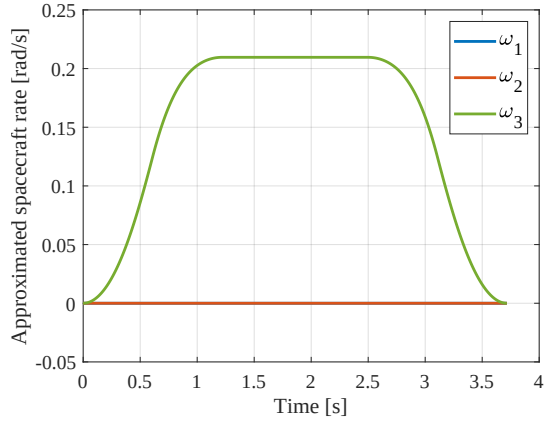

(a) Approximate rate of the spacecraft

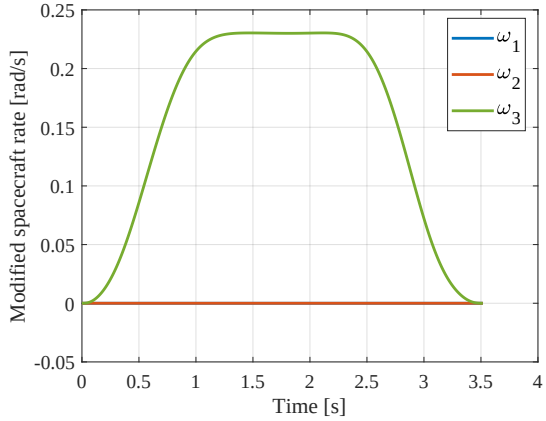

(b) Modified rate of the spacecraft

Fig. 9. Approximate and modified results of trajectories

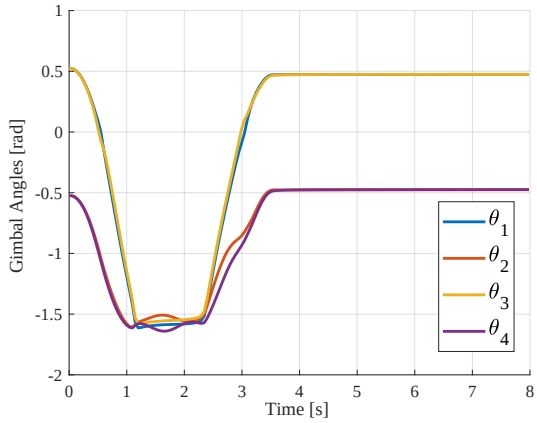

(a) The gimbal angles

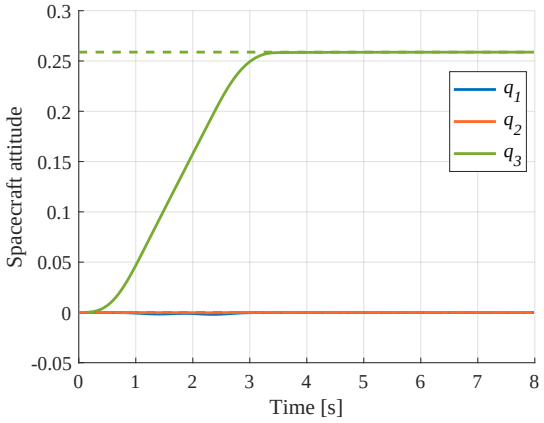

(b) The attitude of the spacecraft

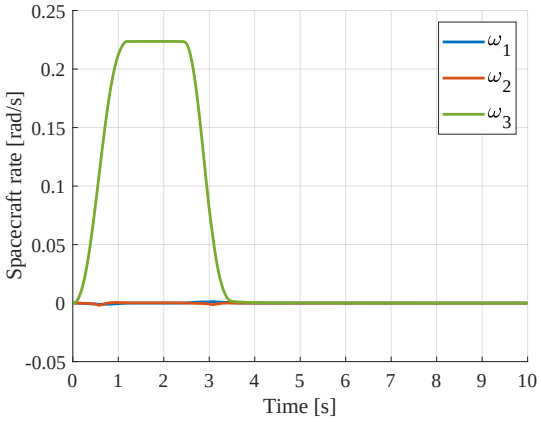

(c) The rate of the spacecraft

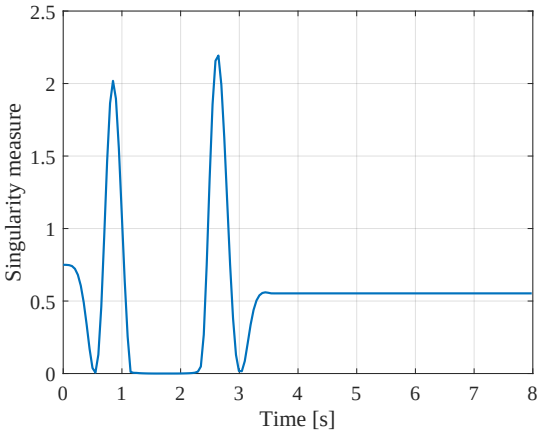

(d) Singularity measure

Fig. 10. Simulation results of attitude control